analytical chemistry

Article

Cite This: *Anal. Chem.* 2019, 91, 4429–4435

pubs.acs.org/ac

Composition Determination of Low-Pressure Gas-Phase Mixtures by ^{1}H NMR Spectroscopy

Christopher L. Suiter, Mark O. McLinden, Thomas J. Bruno, and Jason A. Widegren*

Applied Chemicals and Materials Division, National Institute of Standards and Technology, 325 Broadway, Boulder, Colorado 80305-3328, United States

Supporting Information

ABSTRACT: ^{1}H NMR spectroscopy was used to analyze gas-phase mixtures of methane and propane at pressures near 0.1 MPa. The mixtures were prepared gravimetrically and had low uncertainty in their composition. The primary mixture used for this work had a methane mole fraction of $x_{methane,grav}$ = (0.506875 ± 0.00019) and a propane mole fraction of $x_{propane,grav}$ = (0.493125 ± 0.00019). NMR samples were prepared in two types of commercially available sample tubes that seal with a PTFE piston. Sample pressures ranged from 0.02 to 0.5 MPa. An analysis of measurement uncertainty for the NMR method resulted in combined standard uncertainties that decreased from 0.0082x to 0.0010x, as the pressure increased from 0.02 to 0.5 MPa. The larger uncertainties at lower pressures were primarily caused by uncertainties associated with phasing and baseline correction. A key difficulty in working with gas-phase samples, especially at lower pressures, is that the spectral peaks are inherently broad. Consequently, peak overlap was problematic, and it was not always possible to integrate a high percentage of a peak's intensity. However, with corrections to the integrated areas, based on the assumption of ideal Lorentzian peak shapes, excellent agreement between the NMR analyses and the gravimetric composition was observed across the entire pressure range. These experiments demonstrate the potential of ^{1}H NMR for quantitative composition determinations of low-pressure gas-phase mixtures.

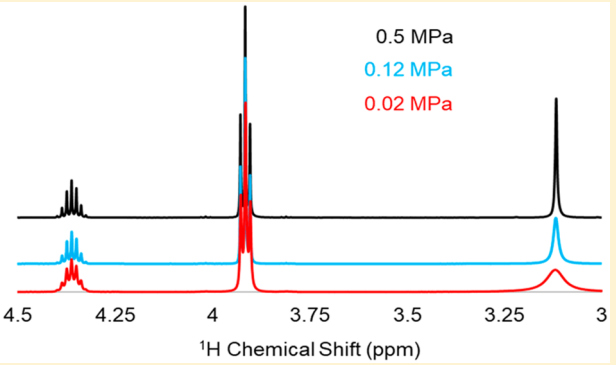

NMR spectroscopy is widely used for quantitative analysis of liquid-phase mixtures.[1−13] ^{1}H NMR is particularly valuable for this purpose because it is relatively easy to collect spectra with high signal-to-noise ratios in which the NMR signals are proportional to the number of nuclei that contribute to the signal.[14] It is well-known that, to achieve a quantitative NMR spectrum, certain experimental conditions must be met. These conditions, such as a pulse repetition time that is long compared to the T_1 relaxation time, have been well described in the literature for liquid-phase samples.[15−19] For liquid-phase samples, the best composition determinations have reported relative standard uncertainties as low as 0.1%.[20]

Despite its wide use for the analysis of liquid-phase mixtures, NMR spectroscopy has been used to analyze gas-phase mixtures in only a few cases.[21−33] Of those, only one study tested the accuracy of the method with a well-defined gas mixture,[23] and that study was also the only one that reported measurement uncertainties for the NMR analysis. In that work, a gravimetrically prepared, 10-component natural gas surrogate (with light hydrocarbons ranging from methane to hexane, as well as CO_2) was analyzed. Because of the complexity of the mixture and the similarity of the mixture components, severe peak overlap was observed in the ^{1}H spectrum; hence, the ^{13}C spectrum had to be used for the composition determination. Due to the low sensitivity of NMR spectroscopy for natural-abundance ^{13}C, high sample pressure (4.4 MPa) and multiple days of signal averaging were needed to collect spectra with sufficient signal intensity for quantitation. Other reports on gas-phase mixture analysis by NMR spectroscopy have not carefully considered measurement uncertainties but have used ^{1}H or ^{19}F, which are more favorable nuclei for quantitation.

The goals for our experiments were to optimize composition determinations for simple gas-phase mixtures with pressures near 0.1 MPa by ^{1}H NMR spectroscopy, and to provide a thorough analysis of the measurement uncertainty. As detailed in the Results and Discussion section, gas-phase samples present multiple difficulties for analysis by NMR spectroscopy, especially at lower pressures. However, with sample pressures near 0.1 MPa, measurements can be made in a standard NMR probe with inexpensive, commercially available sample tubes. Gravimetrically prepared mixtures of methane and propane were chosen for this work for multiple reasons. First, both compounds are stable and are available in high purity, so mixtures with low uncertainty in composition could be

Received: October 29, 2018
Accepted: March 4, 2019
Published: March 4, 2019

DOI: 10.1021/acs.analchem.8b04955
Anal. Chem. 2019, 91, 4429–4435

prepared. Second, the vapor pressures of both components are high enough to avoid condensation in the targeted pressure and temperature range. Third, the ^{1}H spectrum of the mixture has enough peak separation so that peak deconvolution is not required. Fourth, the differing peak widths and multiplicities of the methane and propane signals made it a good test case for data manipulation procedures, such as peak integration.

This work demonstrates that ^{1}H NMR spectroscopy can be used to rapidly and accurately determine molar ratios in simple gas mixtures at total pressures as low as 0.02 MPa (and partial pressures as low as 0.01 MPa). Important applications of this method can be envisioned. The use of NMR for vapor−liquid equilibrium (VLE) measurements has been suggested,[26] and in fact, we are currently using ^{1}H NMR spectroscopy to collect VLE data for binary refrigerant mixtures. NMR spectroscopy can also be used to monitor competitive adsorption,[26,27] permeation,[34] or reaction[21,22,24,25,27,29,30,35] of gas-phase mixtures in real time.

EXPERIMENTAL SECTION

Gas Mixtures. The gravimetrically determined mole fractions of methane and propane in the primary mixture used in this work were $x_{methane,grav} = 0.506875 \pm 0.00019$ and $x_{propane,grav} = 0.493125 \pm 0.00019$. Unless otherwise stated, it is this "50:50 mixture" that was used. Complete sample preparation details from Richter and McLinden[36] are reproduced in the Supporting Information.

Preparation of NMR Samples. Two types of commercially available NMR sample tubes were used for this work, a "low-pressure" tube was used in the pressure range from 0.02 to 0.12 MPa, and a "high-pressure" tube was used in the pressure range from 0.083 to 0.50 MPa. Both types of tubes were sealed with a greaseless PTFE piston. NMR samples were prepared on a simple vacuum manifold that was constructed around a central cross. The four arms of the cross led to a vacuum pump, a pressure transducer, a sample supply tank, and an attachment point for the NMR sample tube. A more detailed description of the sample tubes and the vacuum manifold is available in the Supporting Information.

Acquisition of NMR Spectra. Unless otherwise noted, NMR spectra were acquired within an hour of sample preparation. All NMR experiments were performed at 298.15 K on a commercially available 14.1 T spectrometer (operated at a ^{1}H frequency of 600.130 MHz) with a cryogenic probe. Samples were shimmed manually,[37] taking care to maximize the area of the free induction decay and the line shape of the resonances. Optimal shim settings depended on sample pressure. After shimming, the peak shapes were checked with an automated peak-fitting routine that utilized a combination of Lorentzian and Gaussian functions. In all but two spectra, the optimized peak fit weighted the Lorentzian function ≥0.98 for the central peaks. After shimming, the T_1 relaxation time was determined for each peak using an inversion−recovery pulse sequence.[38]

To obtain quantitative spectra, a high-power, rectangular, 90° pulse was used. The 90° pulse width for ^{1}H was optimized at each nominal pressure, and it ranged from 15 to 17 μs. For each spectrum, 32k data points were collected. The spectral width was 9.02 ppm (5411 Hz), and the offset frequency was adjusted so that the group of three peaks was centered in the spectrum. The prescan delay was 15 μs. The acquisition time was 3.03 s, and the relaxation delay varied from 15 to 38 s (to ensure that the pulse repetition time was ≥10 times the longest T_1 in the sample). Since four scans were used for all quantitative experiments, the total spectral acquisition period ranged from 72 to 164 s; consequently, the effect of the magnetic field drift was negligible.

Processing of NMR Spectra. Data sets were zero-filled to 64k points. Exponential line broadening of 0.3 Hz was applied. After greatly expanding the y-axis of the spectrum, the phase of the peaks was adjusted manually to obtain purely absorptive peaks. A variety of automatic phasing routines were tested, but none were found to work well for all the spectra. Several manuscripts have discussed the importance of phasing with regards to quantitation in NMR.[14,18,39,40] Rabenstein and Keire[14] and Derome[39] suggest that a 5° phase offset in the spectrum will result in a 1% error in the integral value, but it is not clear how broadly this can be applied. Consequently, we estimated the effect of phasing on the uncertainty of the mole fraction determination in the following way. A well phased spectrum for each sample was altered with the zero-order phase until the phasing was obviously dispersive. Then the integrals from these poorly phased spectra were used to calculate mole fractions. The average observed difference in the mole fraction determination at each nominal pressure, between well phased and poorly phased spectra, was taken to correspond to a 99.7% confidence interval for the measurement uncertainty associated with manual phasing (u_{phase}). For the mole fraction determinations, u_{phase} was the dominant source of measurement uncertainty. The relative magnitude of u_{phase} increased at lower pressures; u_{phase} was $0.0079x_{methane}$ for the 0.02 MPa samples and $0.0008x_{methane}$ for the 0.5 MPa samples (for the 50:50 mixture, uncertainties in $x_{methane}$ and $x_{propane}$ are essentially identical).

Broad peaks are problematic for baseline correction methods because any imperfection in the baseline correction is multiplied by the integral width and because of the tendency of such corrections to preferentially remove intensity from broad peaks. We employed a multipoint baseline correction routine with a fourth-order polynomial correction curve. With this method, as with integration (see below), it is necessary to consider line widths (fwhm). Specifically, it is advisable to select baseline points that are at least hundreds of line widths from any peak. The uncertainty caused by baseline drift (u_{bd}) in the corrected baseline was estimated by integrating regions of baseline with the same widths as the integrals used for the spectral peaks. The uncertainty caused by preferential removal of intensity from broad peaks (u_{bc}) was estimated by selecting baseline points at different distances from the spectral peaks (see the Supporting Information for more details).

Other Sources of Measurement Uncertainty. The integral-width correction (see the Results and Discussion section) has some uncertainty due to uncertainty in the line width determination (u_{lw}); the Supporting Information describes how u_{lw} was determined. The peak-overlap correction (see the Results and Discussion section) also has some uncertainty due to uncertainty in the line width determination, but the correction itself is so small ($\leq 0.0008x$) for the 50:50 mixture that the uncertainty in the correction was negligible. Additional sources of measurement uncertainty have been well described for liquid-phase samples and have similar effects on gas-phase samples. Examples of these include T_1 (u_{T1}), digital resolution (u_{res}), frequency offset effects (u_{exc}), receiver gain, pulse calibrations, and others. Additional details about the impact of these effects on measurement uncertainty are presented in the Supporting

DOI: 10.1021/acs.analchem.8b04955
Anal. Chem. 2019, 91, 4429−4435

Information. Each individual source of uncertainty was added in quadrature, in accordance with the Guide to the Expression of Uncertainty in measurement,[41] and the resulting combined standard uncertainties are shown in the figures and tables. The signal-to-noise ratio was sometimes treated as an independent source of measurement uncertainty in NMR experiments.[19,42] Our largest sources of measurement uncertainty, manual phasing (u_{phase}) and baseline correction (u_{bc} and u_{bd}), increased as the signal-to-noise ratio decreased (i.e., as the pressure decreased). We propose that these effects are the dominant factors that contribute to what other researchers identify as uncertainty from the signal-to-noise ratio.

RESULTS AND DISCUSSION

Differences in the Analysis of Gas-Phase Mixtures and Liquid-Phase Mixtures. In general, the approach used for mole fraction determinations on low-pressure, gas-phase mixtures is similar to the approach used for liquid-phase mixtures. However, there are a few important differences associated with gas-phase samples. First, sample preparation and storage are more complicated. Second, there is no deuterated solvent. Third, both T_1 and T_2 relaxation times are strongly dependent on pressure, although different trends are observed for T_1 and T_2.[28,43−45] These differences are occasionally advantageous, but for the most part, they complicate accurate mole fraction determinations. Each of these differences is discussed in greater detail below.

As described in the Experimental Section, samples were prepared in commercially available NMR sample tubes by use of a vacuum manifold. The "high-pressure" tubes had considerably thicker walls, which reduced the internal volume (and thus sensitivity) by almost a factor of 4 compared to the "low-pressure" tubes. Consequently, the low-pressure tubes yielded significantly better data at the lower end of the pressure range. We found it necessary to do a routine leak check when connecting either type of sample tube to the vacuum manifold because that connection was not reliable. The leak check, along with multiple fill-and-evacuate cycles, resulted in a total sample preparation period of about 40 min.

Obviously, gas-phase samples fill the entire sample tube. This is an advantage compared to liquid-phase samples in that sample fill height (which can influence sensitivity, shimming, and repeatability[19]) is not a concern for gas-phase samples. On the other hand, gas-phase samples are in direct contact with every part of the sample tube, which can lead to problems with sample storage and with temperature/density gradients. Due to the design of NMR sample thermostats, a gas-phase sample in a full-length (17 cm) NMR tube experiences a temperature/density gradient.[46] Control experiments (described in the Supporting Information) showed that these gradients did not influence the mole fraction determination for the methane−propane samples. However, when using full-length tubes, such gradients make it imperative to perform mole fraction determinations at temperatures that are well above the dew point of the mixture so that condensation does not occur. For storage, sample sorption caused by PTFE[47−49] and sample leakage were concerns. Therefore, it is noteworthy, that the high-pressure and low-pressure sample tubes yielded the same results within the measurement uncertainty at 0.08 MPa (see Table 1), despite differences in surface area and design. Additionally, long-term tests of sample stability did not reveal any problems for the methane−propane sample in the sample tubes that we employed. For example, Figure 1 shows that, for a sample at a pressure of 0.0885 MPa in a low-pressure tube, the mole fraction determination did not change significantly

Table 1. Mole Fractions of Methane ($x_{methane}$) Determined by ^{1}H NMR Spectroscopy as a Function of Sample Pressure (P)[a]

sample tube	P (MPa)	$x_{methane}$
low-pressure	0.0184	0.5043
low-pressure	0.0190	0.5046
low-pressure	0.0191	0.5056
low-pressure	0.0418	0.5060
low-pressure	0.0423	0.5061
low-pressure	0.0436	0.5059
low-pressure	0.0829	0.5060
low-pressure	0.0833	0.5053
low-pressure	0.0840	0.5062
low-pressure	0.1184	0.5061
low-pressure	0.1195	0.5055
low-pressure	0.1180	0.5064
high-pressure	0.0843	0.5065
high-pressure	0.0839	0.5088
high-pressure	0.0843	0.5060
high-pressure	0.2117	0.5063
high-pressure	0.2126	0.5073
high-pressure	0.2116	0.5072
high-pressure	0.3138	0.5066
high-pressure	0.3136	0.5077
high-pressure	0.3184	0.5073
high-pressure	0.4151	0.5080
high-pressure	0.4178	0.5077
high-pressure	0.4178	0.5085
high-pressure	0.5004	0.5071
high-pressure	0.4988	0.5074
high-pressure	0.4992	0.5073

[a]The standard uncertainty in P is 0.0007 MPa. The standard uncertainty for $x_{methane}$ at each nominal pressure is given in Table 2. The methane−propane mixture used for these measurements was prepared gravimetrically to contain $x_{methane,grav}$ = 0.506875 ± 0.00019.

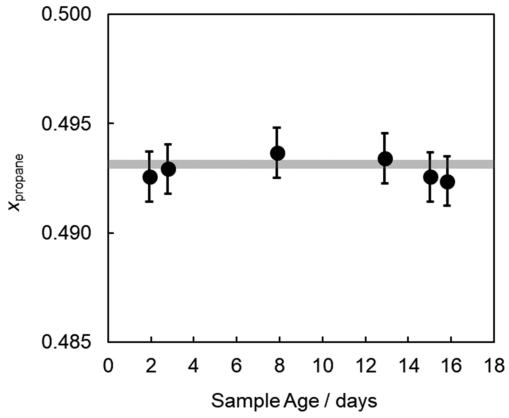

Figure 1. Storage stability of a methane-propane sample at a pressure of 0.0885 MPa in a low-pressure tube. Over the course of 16 days, the mole fractions of propane ($x_{propane}$, shown here) and methane were determined six times by ^{1}H NMR spectroscopy. The NMR-determined mole fractions did not change significantly during this period and were always in good agreement with the gravimetrically determined value. The error bars show the combined standard uncertainty in the NMR measurement, and the width of the gray line shows the uncertainty in the gravimetric value.

DOI: 10.1021/acs.analchem.8b04955
Anal. Chem. 2019, 91, 4429−4435

over the course of 16 days of sample storage. However, when ~1.5 g of additional PTFE was placed inside a low-pressure sample tube, significant changes in sample composition were observed over the same time frame (see the Supporting Information for more details). The impact of the preferential sorption of sample components is expected to be most problematic at low sample pressures, where even low levels of sorption can significantly shift sample composition. In short, when working with gas-phase samples, it is important to test for sample stability, and it is advisable to minimize sample contact with porous materials (including most polymers).

Because of the lack of a deuterated solvent, automatic shimming and frequency locking were not used in this work. The lack of a frequency lock was not a problem for the system studied herein. With a relatively high-field magnet and a cryogenic probe, acceptable signal-to-noise ratios were achieved in less than 3 min, even at the lowest pressure. Consequently, field drift did not significantly affect peak shape. Of course, in cases where much signal averaging is necessary,[23] field drift can be troublesome. The lack of a deuterated solvent was more problematic from the standpoint of shimming. At each nominal pressure, a tedious manual shimming process[37] was used to optimize the shim settings for both peak shape and intensity. This was necessary because good peak shapes are required for the integral-width and peak-overlap corrections that were done as part of the data analysis (see below). Of course, if desired, it is possible to use a deuterium-containing external reference that is contained in a sealed capillary or a coaxial tube.[44,46] The advantages of this approach include the ability to use automated shimming and frequency locking. The disadvantages include a reduction in the volume of gas-phase sample in the active region of the NMR tube and the need to do peak-overlap corrections for the reference peaks. An experiment with a methane−propane sample and a sealed capillary containing D_2O is described in the Supporting Information.

For spin-1/2 nuclei in polyatomic gases, the T_1 relaxation time constant is longest at very high densities (i.e., at high pressures) and very low densities; at intermediate densities, T_1 passes through a minimum.[28,43−45] This behavior makes it necessary to determine the relevant values of T_1 at each pressure to ensure that the delay between pulses is long enough for (nearly) complete signal recovery. Near 0.1 MPa, values of T_1 for gas-phase samples are generally short, especially for small, symmetric molecules.[43,44] This is an advantage for quantitative work because it shortens the time required to collect spectra. The observed values of T_1 were longest at 0.5 MPa, decreased as the pressure decreased to 0.04 MPa, and then increased slightly at 0.02 MPa. This suggests that the pressure range used for this study was near the (optimal) minimum from the standpoint of T_1. It is advantageous if the spin-rotation mechanism of relaxation is similar for the different components of the mixture. This leads to a similar behavior in T_1 relaxation times, which facilitates the acquisition of quantitative spectra.

The T_2 relaxation time constant is not commonly measured for gas-phase samples; however, for spin-1/2 nuclei in polyatomic gases, T_2 is expected to decrease with decreasing density in the range studied herein.[1,9,43,44] The observation of broader line widths at lower pressures is consistent with this expectation. Figure 2 shows the magnitude of this effect. As described below, proper handling of the integration of broad peaks was a key to achieving low uncertainties at low pressure.

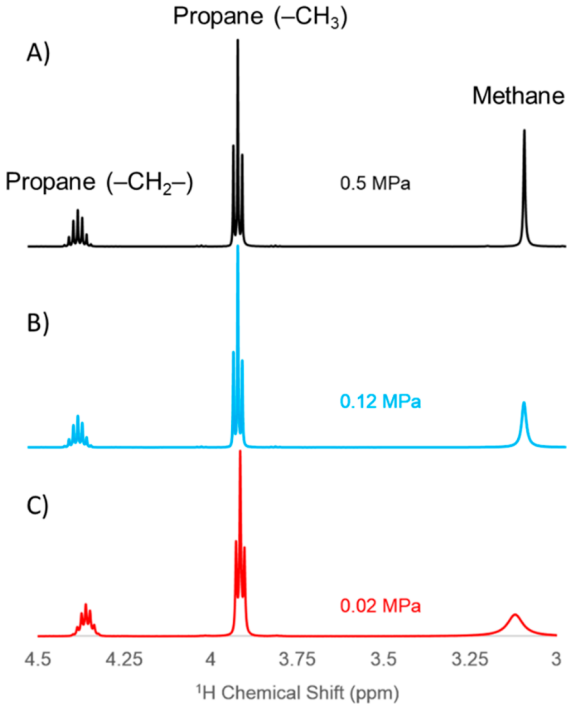

Figure 2. NMR spectra for methane−propane samples at (A) 0.5, (B) 0.12, and (C) 0.02 MPa. The line width (fwhm) for the methane peak is about an order of magnitude broader at 0.02 MPa than at 0.5 MPa.

Systematic Approach for the Integration of Broad Peaks. Lorentzian peaks can be described as a function of line width. The signal intensity for an ideal Lorentzian peak shape is described by the probability density function

$$f(x; x_0, \gamma) = \frac{1}{\pi\gamma}\left[\frac{\gamma^2}{(x - x_0)^2 + \gamma^2}\right] \quad (1)$$

where x_0 is the location of the peak maximum, and γ is the half-width at half of the maximum signal intensity (therefore, the fwhm is 2γ). If the peak maximum is set at zero (i.e., $x_0 = 0$ Hz), and the fwhm is set at 2 Hz (that is, $\gamma = 1$ Hz), then the function simplifies to

$$f(x; 0, 1) = \frac{1}{\pi(1 + x^2)} \quad (2)$$

Like all probability distribution functions, eqs 1 and 2 integrate to 1.0 if the integral limits are set to $-\infty$ and $+\infty$. Hence, narrower integral limits can be used to determine the fraction of peak intensity within a chosen number of line widths on either side of the peak maximum. Integration of eq 2 with limits of $-\infty$ to x gives

$$f(x; 0, 1) = \frac{\arctan(x)}{\pi} + 0.5 \quad (3)$$

which is the fraction of the peak area from $-\infty$ to x. To obtain the normalized area fraction between any two limits, one subtracts the value of eq 3 at the lower limit from the value of eq 3 at the higher limit. Table S1 is a list of peak area fractions vs the number of line widths integrated for whole-number, symmetric, integral ranges up ±400 line widths.

For quantitative experiments, it is imperative to know what fraction of each peak has been integrated. For example, to capture 99.9% of the total peak intensity, one must integrate

DOI: 10.1021/acs.analchem.8b04955
Anal. Chem. 2019, 91, 4429−4435

Table 2. Uncertainty Budget at Each Nominal Sample Pressure (P)

		relative standard uncertainties[a]							
sample tube	P (MPa)	u_{phase} (%)	u_{bc} (%)	u_{bd} (%)	u_{lw} (%)	u_{exc} (%)	u_{res} (%)	u_{T1} (%)	u_c[b] (%)
low-pressure	0.02	0.79	0.22	0.08	0.04	0.04	0.01	0.005	0.82
low-pressure	0.04	0.37	0.04	0.04	0.05	0.04	0.01	0.005	0.38
low-pressure	0.08	0.21	0.04	0.03	0.08	0.04	0.01	0.005	0.23
low-pressure	0.12	0.13	0.06	0.01	0.08	0.04	0.01	0.005	0.18
high-pressure	0.08	0.33	0.22	0.08	0.03	0.04	0.01	0.005	0.41
high-pressure	0.2	0.20	0.12	0.02	0.08	0.04	0.01	0.005	0.25
high-pressure	0.3	0.15	0.10	0.03	0.03	0.04	0.01	0.005	0.19
high-pressure	0.4	0.12	0.08	0.03	0.04	0.04	0.01	0.005	0.16
high-pressure	0.5	0.08	0.04	0.02	0.01	0.04	0.01	0.005	0.10

[a]See the Experimental Section for a detailed description of each source of uncertainty. [b]The combined standard uncertainty (u_c) was calculated by adding the uncertainties in quandrature.

319 line widths on either side of the peak (Table S1). Occasional references to this issue exist in the literature, usually with the conclusion that a certain number of line widths need to be integrated to achieve a certain level of accuracy.[15,50] However, even for narrow spectral peaks, such broad integral ranges are often not possible because of insufficient peak separation. The relatively broad peaks observed for gas-phase samples, especially at lower pressures, greatly exacerbate this problem. Our primary strategy for achieving accurate integral values was to (1) determine the line width of each peak, (2) set an integral range for each peak based on the line width, and (3) then to apply a correction to the integrated area based on the number of line widths integrated. This "integral-width correction" was largest for the lowest pressure samples, where line widths were the broadest. For example, at nominal pressures of 0.02 MPa, where ±30 line widths were integrated for the propane peaks and ±10 line widths were integrated for the methane peak, the integral-width correction shifted the calculated mole fractions by $0.011x$. An illustrated example of the integral-width correction for a methane−propane spectrum is provided in the Supporting Information. For some spectra, it is possible to integrate all peaks of interest with integral regions that contain the same number of line widths;[50] this "equal-line widths strategy" obviates the need for a correction. The equal-line widths strategy was used for all samples with pressures ≥0.3 MPa, but at lower pressures, the methane singlet was too broad for this to be feasible. Although the focus of this article is on gas-phase samples, the integral-width correction (or equal-line widths strategy) can be used for any NMR spectrum with broad or closely spaced peaks. The integral-width correction is also applicable when narrow integral regions are used to minimize the influence of baseline drift.

Because of the shape of Lorentzian peaks, every peak overlaps every other peak in an NMR spectrum; however, the extent of overlap is not always significant. The importance of peak overlap increases rapidly as the relative sizes of the peaks diverge, and as the peaks get closer together (in terms of the number of line widths of separation). The importance of peak-overlap also increases as the integration ranges increase or diverge in terms of the number of line widths integrated. A "peak-overlap correction" was performed in much the same way as the integral-width correction: the extent of overlap was determined from eq 3 (or Table S1) based on the distance (in terms of line widths) between a peak's maximum and a neighboring peak's integral limits; then, the overlapping area was subtracted from the neighboring peak's integrated area. An illustrated example of the peak-overlap correction for a methane−propane spectrum is provided in the Supporting Information. Largely because of similarly sized peaks, the peak-overlap correction is relatively unimportant for the 50:50 mixture; the correction shifted the calculated mole fraction of propane by $\leq 0.0008x_{propane}$. However, for a 75:25 mixture of methane and propane at similar pressures, the peak-overlap correction shifted the calculated mole fraction of propane by as much as $0.012x_{propane}$, which illustrates the importance of relative peak size for this correction.

Effect of Peak Multiplicity on Integration. In spectra with only singlet peaks, the integral-width and peak-overlap corrections require no assumptions beyond a Lorentzian line shape. Multiplet peaks complicate matters because the outer peaks in a multiplet occupy a different position within the integral than the center peak(s), and the individual peaks of a multiplet are typically too close together to be integrated separately. Fortunately, if the integral limits are broad enough, a multiplet can be treated as if it were a singlet without introducing significant error into the integral-width correction or the peak-overlap correction. That is, one assumes that all the intensity of the multiplet comes from a singlet at the center of the multiplet with the same line width as that of the central peak(s) in the multiplet. This "multiplet approximation" was used for the all the data reported in the figures and tables. A validation of the multiplet approximation is provided in the Supporting Information.

Uncertainty of Mole Fraction Determinations as a Function of Pressure. Methane−propane samples were prepared with nominal pressures ranging from 0.02 to 0.5 MPa. The low-pressure tube was used for samples at nominal pressures of 0.02, 0.04, 0.08, and 0.12 MPa. The high-pressure tube was used for samples at nominal pressures of 0.08, 0.2, 0.3, 0.4, and 0.5 MPa. At each nominal pressure, three independent samples of the 50:50 mixture were prepared for NMR analysis. For each measurement that was done, Table 1 shows the NMR-determined mole fraction for methane. Table 2 shows the uncertainty budget and combined standard uncertainty at each nominal sample pressure. The mole fraction of propane for each measurement can be determined by difference (and the uncertainty in $x_{methane}$ and $x_{propane}$ are essentially identical for the 50:50 mixture). Figure 3 is a deviation plot of the same information. The gray band in the center of the plot shows the uncertainty in the composition of the gravimetrically prepared mixture. Of the 27 samples shown in Figure 3 and Table 1, there are only four cases in which the

DOI: 10.1021/acs.analchem.8b04955
Anal. Chem. 2019, 91, 4429−4435

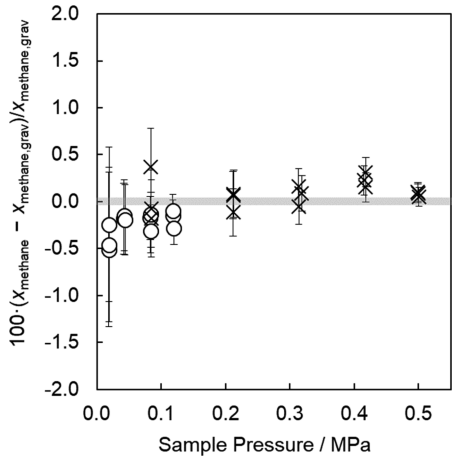

Figure 3. Percent difference between the NMR-determined mole fraction of methane ($x_{methane}$) and the gravimetric value ($x_{methane,grav}$) as a function of sample pressure. ○, low-pressure sample tube; ×, high-pressure sample tube. The error bars show the combined standard uncertainty in the NMR measurement, and the width of the gray line shows the standard uncertainty in the gravimetric value. Excellent agreement was observed across the entire pressure range; out of 27 samples, there are only 4 cases in which the combined standard uncertainty interval for $x_{methane}$ did not overlap the uncertainty interval for $x_{methane,grav}$.

combined standard uncertainty interval for $x_{methane}$ did not overlap the uncertainty interval for $x_{methane,grav}$.

At higher pressures, the integral-width and peak-overlap corrections are less important because the peaks are narrower. For most of the measurements in the high-pressure NMR tubes, the peak-overlap corrections were very small (≤0.02% change in calculated mole fraction at pressures ≥0.2 MPa), and the equal-line widths strategy (see above) was used for integration, so no additional integral-width correction was necessary. However, none of the measurements in the low pressure tubes would overlap the uncertainty interval for $x_{methane,grav}$ without the integral-width and peak-overlap corrections, and deviations as large as 1.6% would be observed at the lowest pressures. Obviously, these corrections were a key to achieving accurate results at low pressure.

CONCLUSIONS

This work demonstrates the utility of ^{1}H NMR spectroscopy for the analysis of simple gas-phase mixtures at pressures near 0.1 MPa. The combined standard uncertainty in the mole fraction determination decreased from 0.0082x to 0.0010x as the pressure increased from 0.02 to 0.5 MPa. The larger uncertainties at lower pressures are primarily caused by uncertainties associated with phasing and baseline correction (both of which are more problematic with lower signal-to-noise ratios and broader peaks). Preferential sorption of sample components was not significant for the measurements presented herein but could be problematic in other systems. A key difficulty in working with gas-phase samples, especially at lower pressures, is that the spectral peaks are inherently broad. This difficulty was surmounted by correcting the integrated peak areas for peak overlap and integral width. With these corrections, uncertainties comparable to the best liquid-phase composition measurements by ^{1}H NMR spectroscopy were achieved. These same corrections can be applied to any NMR spectrum with broad or closely spaced peaks, thus facilitating low-uncertainty mole fraction determinations and qNMR experiments on challenging liquid-phase samples as well. The low uncertainty of ^{1}H NMR spectroscopy for the analysis of gas-phase mixtures could be advantageous for many fields of inquiry. We are currently exploring the use of ^{1}H NMR spectroscopy for high-accuracy measurements of vapor−liquid equilibria.

ASSOCIATED CONTENT

Supporting Information

The Supporting Information is available free of charge on the ACS Publications website at DOI: 10.1021/acs.analchem.8b04955.

Additional experimental details; the fraction of the total peak intensity that is within a given number of line widths on each side of the peak maximum; additional information about the integration of spectral peaks at each nominal pressure; example of the peak-overlap and integral-width corrections; use of the integral-width and peak-overlap corrections with multiplets; use of line fitting to determine peak areas; preferential adsorption of propane by PTFE; results of an independent analysis of all the spectra by a second spectroscopist; use of an external deuterium lock with gas-phase samples; and control experiments related to the use of open, full-length, and NMR tubes for gas-phase samples (PDF)

AUTHOR INFORMATION

Corresponding Author

*E-mail: jason.widegren@nist.gov; Phone: 1 303 497 5207.

ORCID

Jason A. Widegren: 0000-0003-1077-7035

Notes

Contribution of the United States Government; not subject to copyright in the United States.

The authors declare no competing financial interest.

ACKNOWLEDGMENTS

The authors thank Richard Shoemaker (Bruker Biospin) for useful discussions

REFERENCES

(1) Saude, E. J.; Slupsky, C. M.; Sykes, B. D. *Metabolomics* **2006**, *2*, 113−123.

(2) Jones, I. C.; Sharman, G. J.; Pidgeon, J. *Magn. Reson. Chem.* **2005**, *43*, 497−509.

(3) Pauli, G. F.; Chen, S. N.; Simmler, C.; Lankin, D. C.; Godecke, T.; Jaki, B. U.; Friesen, J. B.; McAlpine, J. B.; Napolitano, J. G. *J. Med. Chem.* **2014**, *57*, 9220−9231.

(4) Singh, S.; Roy, R. *Expert Opin. Drug Discovery* **2016**, *11*, 695−706.

(5) Sun, S. S.; Jin, M. X.; Zhou, X.; Ni, J. H.; Jin, X. J.; Liu, H. Y.; Wang, Y. H. The Application of Quantitative 1H-NMR for the Determination of Orlistat in Tablets*Molecules* **2017**, *22*.1517

(6) Tanaka, R.; Inagaki, R.; Sugimoto, N.; Akiyama, H.; Nagatsu, A. *J. Nat. Med.* **2017**, *71*, 315−320.

(7) Wells, R. J.; Hook, J. M.; Al-Deen, T. S.; Hibbert, D. B. *J. Agric. Food Chem.* **2002**, *50*, 3366−3374.

(8) Mello, V. M.; Oliveira, F. C. C.; Fraga, W. G.; do Nascimento, C. J.; Suarez, P. A. Z. *Magn. Reson. Chem.* **2008**, *46*, 1051−1054.

(9) Mambrini, G. P.; Ribeiro, C.; Colnago, L. A. *Magn. Reson. Chem.* **2012**, *50*, 1−4.

DOI: 10.1021/acs.analchem.8b04955
Anal. Chem. 2019, 91, 4429−4435

(10) Ottavioli, J.; Casanova, J.; Bighelli, A. *Spectrosc. Lett.* **2011**, *44*, 221−228.
(11) Muntean, J. V.; Libera, J. A.; Snyder, S. W.; Wu, T. P.; Cronauer, D. C. *Energy Fuels* **2013**, *27*, 133−137.
(12) Mazumder, A.; Kumar, A.; Purohit, A. K.; Dubey, D. K. *Anal. Bioanal. Chem.* **2012**, *402*, 1643−1652.
(13) Pauli, G. F.; Godecke, T.; Jaki, B. U.; Lankin, D. C. *J. Nat. Prod.* **2012**, *75*, 834−851.
(14) Rabenstein, D. L.; Keite, D. A. Quantitative Chemical Analysis by NMR. In *Modern NMR Techniques and Their Application in Chemistry*; Popov, A. I., Ed.; Marcel Dekker: New York, 1991; pp 233−369.
(15) Griffiths, L.; Irving, A. M. *Analyst* **1998**, *123*, 1061−1068.
(16) Saito, T.; Nakaie, S.; Kinoshita, M.; Ihara, T.; Kinugasa, S.; Nomura, A.; Maeda, T. *Metrologia* **2004**, *41*, 213−218.
(17) Malz, F.; Jancke, H. *J. Pharm. Biomed. Anal.* **2005**, *38*, 813−823.
(18) Bharti, S. K.; Roy, R. *TrAC, Trends Anal. Chem.* **2012**, *35*, 5−26.
(19) Le Gresley, A.; Fardus, F.; Warren, J. *Crit. Rev. Anal. Chem.* **2015**, *45*, 300−310.
(20) Weber, M.; Hellriegel, C.; Ruck, A.; Sauermoser, R.; Wuthrich, J. *Accredit. Qual. Assur.* **2013**, *18*, 91−98.
(21) Krusic, P. J.; Roe, D. C. *Anal. Chem.* **2004**, *76*, 3800−3803.
(22) Marchione, A. A.; Fagan, P. J.; Till, E. J.; Waterland, R. L.; LaMarca, C. *Anal. Chem.* **2008**, *80*, 6317−6322.
(23) Meyer, K.; Rademann, K.; Panne, U.; Maiwald, M. *J. Magn. Reson.* **2017**, *275*, 1−10.
(24) Krusic, P. J.; Marchione, A. A.; Roe, D. C. *J. Fluorine Chem.* **2005**, *126*, 1510−1516.
(25) Kating, P. M.; Krusic, P. J.; Roe, D. C.; Smart, B. E. *J. Am. Chem. Soc.* **1996**, *118*, 10000−10001.
(26) Rittig, F.; Aurentz, D. J.; Coe, C. G.; Kitzhoffer, R. J.; Zielinski, J. M. *Ind. Eng. Chem. Res.* **2002**, *41*, 4430−4434.
(27) Ernst, H.; Karger, J. *Z. Phys. Chemie-Leipzig* **1987**, *268*, 321−328.
(28) Roe, D. C.; Kating, P. M.; Krusic, P. J.; Smart, B. E. *Top. Catal.* **1998**, *5*, 133−147.
(29) Costello, F.; Dalton, D. R.; Poole, J. A. *J. Phys. Chem.* **1986**, *90*, 5352−5357.
(30) Shtarov, A. B.; Krusic, P. J.; Smart, B. E.; Dolbier, W. R. *J. Am. Chem. Soc.* **2001**, *123*, 9956−9962.
(31) Nibler, J. W.; Minarik, P.; Fitts, W.; Kohnert, R. *J. Chem. Educ.* **1996**, *73*, 99−101.
(32) Kachala, V. V.; Khemchyan, L. L.; Kashin, A. S.; Orlov, N. V.; Grachev, A. A.; Zalesskiy, S. S.; Ananikov, V. P. *Russ. Chem. Rev.* **2013**, *82*, 648−685.
(33) Haugh, M. J.; Dalton, D. R. *J. Am. Chem. Soc.* **1975**, *97*, 5674−5678.
(34) Wind, J. D.; Paul, D. R.; Koros, W. J. *J. Membr. Sci.* **2004**, *228*, 227−236.
(35) Wennberg, P. O.; Bates, K. H.; Crounse, J. D.; Dodson, L. G.; McVay, R. C.; Mertens, L. A.; Nguyen, T. B.; Praske, E.; Schwantes, R. H.; Smarte, M. D.; St Clair, J. M.; Teng, A. P.; Zhang, X.; Seinfeld, J. H. *Chem. Rev.* **2018**, *118*, 3337−3390.
(36) Richter, M.; McLinden, M. O. *J. Chem. Eng. Data* **2014**, *59*, 4151−4164.
(37) Cavanagh, J. *Protein NMR Spectroscopy: Principles and Practice*, 2nd ed.; Academic Press: Amsterdam, Boston, 2007.
(38) Claridge, T. D. W. *High-Resolution NMR Techniques in Organic Chemistry*, 2nd ed.; Elsevier: Amsterdam, 2009.
(39) Derome, A. E. *Modern NMR Techniques for Chemistry Research*, 1st ed.; Pergamon Press: Oxford Oxfordshire, New York, 1987.
(40) Zientek, N.; Meyer, K.; Kern, S.; Maiwald, M. *Chem. Ing. Tech.* **2016**, *88*, 698−709.
(41) Evaluation of measurement data−Guide to the expression of uncertainty in measurement. *JCGM-100:2008*; JCGM, 2008.
(42) Larive, C. K.; Jayawickrama, D.; Orfi, L. *Appl. Spectrosc.* **1997**, *51*, 1531−1536.
(43) Armstrong, R. L. *Magn. Reson. Rev.* **1987**, *12*, 91−135.
(44) Govil, G. *Appl. Spectrosc. Rev.* **1973**, *7*, 47−78.
(45) Jameson, C. J. *Chem. Rev.* **1991**, *91*, 1375−1395.
(46) Jackowski, K.; Jaszuński, M. *Gas Phase NMR*; The Royal Society of Chemistry: Cambridge, 2016.
(47) Dobson, J. V.; Taylor, M. J. *Electrochim. Acta* **1986**, *31*, 231−233.
(48) Pagonis, D.; Krechmer, J. E.; de Gouw, J.; Jimenez, J. L.; Ziemann, P. J. *Atmos. Meas. Tech.* **2017**, *10*, 4687−4696.
(49) Yiyan, N.; Felder, R. M.; Koros, W. J. *J. Appl. Polym. Sci.* **1980**, *25*, 1755−1774.
(50) Sotak, C. H.; Dumoulin, C. L.; Levy, G. C. *Anal. Chem.* **1983**, *55*, 782−787.

DOI: 10.1021/acs.analchem.8b04955
Anal. Chem. 2019, 91, 4429−4435